Studies on the Reduction Rate of Aromatic Nitrocompounds by Bechamp's Method

By Sakae YAGI, Terukatsu MIYAUCHI and Chia You YEH

(Received August 2, 1955)

I. Introduction

Since 1854, the year in which Béchamp reduced aromatic nitrocompounds to corresponding primary amino-compounds using iron particles and acetic acid, many investigations into Bechamp's reduction have been carried out by various authors[1] from the scientific and technical standpoints. The curious catalytic action of hydrochloric acid which came into use later was investigated by Witt[2], Whol[3], Raikow[4] and others.

Effective catalysts for the reaction were greatly extended in their scope by Lyons and Smith[5], and recently the reaction mechanism has been discussed by Luder and Zuffanti[6] from the electronic point of view.

Technical preparations of primary amines by this method are now generally performed by batchwise operation.

Some investigations[7] into a continuous process have been reported in the literature, but their industrial success is yet uncertain. With the same purpose as mentioned above, we have studied the technical reaction rate of this reduction as a fundamental approach to an industrially feasible continuous operation. No systematic data on the reaction rate seem to have been published yet.

First, we investigated a batchwise process using an agitated vessel and later a continuous process by means of a fluidized bed reactor proposed by one of the authors[8]. Studies reported here only cover the former.

II. Experimental Procedures

Fig. 1 illustrates the assembly of the reactor. The reaction vessel is composed of double cylindrical tanks, both made of mild steel. The dimensions of the inner part are 100 mm. dia. × 114 mm. height (about one liter in volume). The annular space between the tanks is filled with a boiling liquid as a heat-transfer medium, choice being made among water, methanol, ethanol and a mixture of water and ethanol, each for its own reaction temperature.

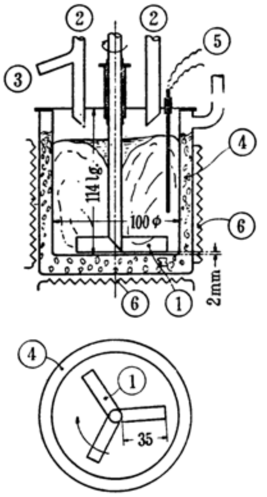

Fig. 1. Experimental apparatus.
1. Three-blades impeller.
2. Reflux condenser.
3. Sampling tube for condensate.
4. Constant-temperature bath.
5. Thermocouple.
6. Electric heatee.

Two reflux condensers at the upper part of the reactor and a sampling tube, to obtain samples of refluxing condensate for analysis, are arranged as shown in the figure.

An impeller composed of three brass blades and a mild steel shaft (blade length 35 mm., blade width 13 mm., blade inclination to the horizontal plane 30° and diameter of the shaft 10 mm.) is rotated in the inner vessel at the axial position, with variable speed.

After the temperature is raised to the desired point, weighed aqueous hydrochloric acid solution of known concentration and weighed iron particles are introduced into the reaction vessel and agitated. When evolution of hydrogen gas ceases about three or four minutes later, the weighed nitrocompound preheated to the reaction temperature is introduced as fast as possible within about 20 sec. The lapse of time from the completion of the introduction to the sampling is regarded as the reaction time. Prior to the runs, the iron particles are pretreated as follows. To remove oily matter, the particles are kept in a loosely closed glass flask and exposed to the

---

[1] P.H. Groggins, "Unit process in Organic Synthesis", McGraw-Hill Pub. Co., 4th ed., (1952).

[2] O.N. Witt, *Chemische Ind.*, **10**, 218 (1887).

[3] A. Wohl, *Ber.*, **27**, 1432, 1815 (1894).

[4] P.N. Raikow, *Zeit. für Angew. Chem.*, **26**, 196, 239 (1916).

[5] R.E. Lyons and L.T. Smith, *Ber.*, **60**, 173 (1927).

[6] W.F. Luder and S. Zuffanti, refer to 1), p. 89.

[7] A.G. Kalle, (I.G.), *Ind. Eng. Chem.*, **40**, 1574 (1948); Vikman and Mukhanova, Russian p. 52006 (1937).

[8] Sakae Yagi, Japanese pat. 204, 536 (1954).

temperature of 450°C for ninety minutes. They are cooled and then etched with dilute hydrochloric acid. Nitrobenzene and hydrochloric acid are respectively of "extra-pure grade" and the other nitrocompounds are of "chemically-pure grade".

III. Analytical Methods

Liquid mixtures such as $PhNO_2$–$PhNH_2$–H_2O or *o*-nitrotoluene-*o*-toluidine-water are analysed under ordinary temperature as follows:

Provided the value of Φ, the molar ratio of the residual nitrocompound to its initial quantity, is higher than about 0.1, a fairly good linearlity holds between amine mole fraction, in an equilibrium mixture of three components, and its refractive index, as shown in Fig. 2. Then with a small quantity of refluxing condensate taken at intervals, its refractive index is measured with an Abbe Refractometer after separating the sample into two liquid layers by a centrifuge. The true value of Φ can then be determined from the equilibrium relationship between composition of the refluxing condensate and that of the bulk.

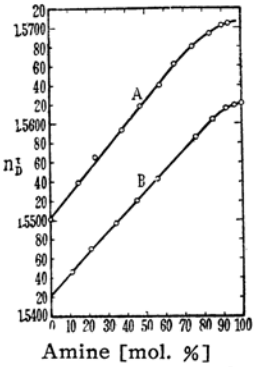

Fig. 2. Refractive index vs. Φ.

(a) Ph. NO_2–Ph. NH_2–H_2O System at 42.5°C.

(b) ortho. $CH_3C_6H_4NO_2$ –ortho. $CH_3C_6H_4NH_2$–H_2O at 25.0°C.

A polarographic determination⁹⁾ is made when Φ is smaller than 0.05 because the linearlity does not hold in this range. Samples are taken from liquid bulk in this case.

p-nitrotoluene and α-nitronaphthalene are determined by volumetric analysis since their reaction mixtures remain in solid state under ordinary temperatures.

During reduction, a few ml. of the oil layer is taken from the liquid bulk, neutralized with a saturated aqueous solution of sodium carbonate and diluted with a known quantity of ethanol.

Analysing this filtrate, total amine and nitrocompound are determined respectively. The former is back-titrated¹⁰⁾ with 0.1 N sulfanilic acid solution after an excess of 0.1 N sodium nitrite solution is added. The reduction method¹¹⁾ with $TiCl_3$ is employed to determine the content of nitro-compound.

IV. Expression of the Reaction Rate

As will be later described, it is experimentally found out that the reaction rate is proportional to the surface area of iron, provided the iron particles are fully fluidized into the reaction mixture.

The overall reaction rate, R is expressed as the rate of nitrocompound consumption per unit surface area of active iron, as

$$R=-\frac{1}{A_T}\frac{\mathrm{d}N_N}{\mathrm{d}\theta}=-\frac{1}{a_T}\frac{\mathrm{d}\Phi}{\mathrm{d}\theta}$$

$$=-\frac{1}{a_p+a_w}\frac{\mathrm{d}\Phi}{\mathrm{d}\theta} \tag{1}$$

where R=Overall reaction rate (mol./cm²min.)

θ=Reaction time (min.).

$A_T=(A_p+A_w)$, the total surface area of reacting iron after the lapse of time θ (cm²).

A_p=Surface area of iron particles after θ (cm²).

A_w=Inside wall area of the reaction vessel plus the surface area of mild steel shaft both of which keep contact with the reaction mixture (cm²).

N_{N_0}=Initial molal quantity of nitrocompound (mol.).

N_N=Residual molal quantity of θ nitrocompound after θ (mol.).

$$\Phi=N_N/N_{N_0}\,,\quad a_T=A_T/N_{N_0}=a_p+a_w\,,$$
$$a_p=A_p/N_{N_0}\,,\quad a_w=A_w/N_{N_0}$$

From the material balance between reactants, N_F, the residual atomic quantity of iron particles after θ, is given by Eq. (2), with an assumption that the overall stoichiometric chemical equation is as follows since hydrochloric acid behaves ultimately as a catalyst

$$R\cdot NO_2+H_2O+\frac{9}{4}Fe=R\cdot NH_2+\frac{3}{4}Fe_3O_4$$

$$N_F=N_{F_0}-\frac{9}{4}\left\{(N_{N_0}-N_N)-\int_0^\theta A_w R\,\mathrm{d}\theta\right\} \tag{2}$$

where N_{F_0} is the initial atomic quantity of iron particles (atms).

On the other hand, F_p, the weight of iron particles after θ, and A_p are assumed to be expressed by Eqs. (3) and (4) respectively

$$F_p=\psi\rho_F d_p^3 n=N_F M_F \tag{3}$$

---

9) T. Takeuchi and M. Kasaki, *J. Soc. Chem. Ind. Japan*, **52**, 69 (1949).

10) J. Phillips and A. Lowy, *Ind. Eng. Chem., Anal. Ed.*, **9**, 381 (1937).

11) F.L. English, *Ind. Eng. Chem.*, **12**, 994 (1920).

$$A_p=\phi d_p^2 n \tag{4}$$

where M_F = Atomic weight of Fe (g./mol.).
ρ_F = True density of iron (g./cm^3).
d_p = Mean representative diameter of iron particles after θ (cm.).
n = Total number of iron particles (—).
ψ = Volumetric shape factor (—).
ϕ = Surface shape factor (—).

From the Eqs. (2), (3) and (4), a_p or A_p/N_{N0} is finally transformed into Eq. (5), provided the ratio of ϕ to ψ remains fairly constant or its mean value maintained throughout the progress of the reaction.

$$a_p=\frac{\phi}{\psi\rho_F}\cdot\frac{M_F\beta}{d_{p0}}\left[1-\frac{9}{4\beta}\left\{(1-\Phi)-\int_0^\theta a_w R\mathrm{d}\theta\right\}\right]^{2/3} \tag{5}$$

where $\beta=N_{F0}/N_{N0}$
d_{p0} = Mean representative diameter of iron particles at the beginning (cm.).

By means of Eqs. (1) and (5), we are able to express the experimental data in terms of R.

For practical calculations, however, the term $\int_0^\theta a_w R\mathrm{d}\theta$ is inconvenient to use. Therefore, from equation (1) we obtain

$$R\mathrm{d}\theta=-\mathrm{d}\Phi/(a_p+a_w)$$

and which enables us to transform the above integral into:

$$\int_0^\theta a_w R\mathrm{d}\theta=\int_\Phi^{1.0}\frac{\mathrm{d}\Phi}{1+a_p/a_w}$$

This final form is used to correct the surface effect of iron vessel and agitator shaft.

In order to calculate a_p, by Eq. (5), based on the experimental data, the integral in the parentheses is neglected at first, as the first approximation, and R is calculated based on this approximation. With this approximate value of R, a_p is recalculated by Eq. (5) as the second approximation. Such recalculations are repeated until the final value of R is obtained.

In our experiments, the value of A_w is 210 cm^2 and the ratio of a_w/a_p, in one of our runs, is 2.72% at the initial stage of reaction and 10.1% at the final stage, provided the β- value is 2.50. The mean representative diameter of the iron particles is defined as the geometrical mean value of the upper and lower sizes of mesh, and the ratio of the shape factors is determined by microscopic observation.

V. Reduction of Nitrobenzene by Bechamp's Method

Because of the fundamental importance of nitrobenzene among various nitrocompounds, basic studies are mainly centered on the reduction of this compound.

V-1. Effects of Various Physical Factors. —In this reaction, the system is composed of a mixture of four heterogeneous phases of solid iron particles, oxide sludge, an acidic aqueous layer and an oil layer. Experiments are made to determine in which phase or phase boundary the reaction proceeds mainly.

a. Effect of Rotation Speed of the Impeller. —Rotation speed of the mixing impeller mainly has influences on fluidization of iron particles into liquid bulk (settling of iron particles results in decrease in effective reaction surface), diffusional rate of reactants to the surface of iron particles, dispersion of heterogeneous liquid phases, mass transfer rate between these phases, removal and control of reaction heat and equalization of reaction temperature within the reaction mixture.

Under a standard reaction condition (refer to V–3), the rotation speed of the impeller is set at 550, 1100 and 2200 r.p.m. Between 800 and 900 r.p.m., there is a critical rotation speed where the total iron particles are fully fluidized into the liquid bulk.

The reaction rate at Φ-value of 0.5 (the rate around this Φ-value is apparently expressed by zeroth-order reaction) is illustrated in Fig. 3.

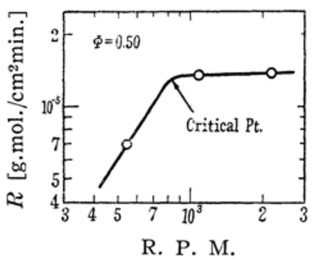

Fig. 3. R vs. r.p.m.

As obvious from the figure, the effect due to the rotation speed of the stirrer on the reaction rate is negligible when the iron particles are fully fluidized into the liquid bulk or the total surface area of iron particles is all effectively used.

For this reason, all the subsequent runs are performed at the rotation speed of 1100 r.p.m.

b. Effect of Surface Area of Iron Particles on the Reaction Rate.—Under the standard reaction conditions, experiments are made to trace the effect of surface area of iron particles on the reaction rate. A method of varying β with constant mesh size of iron particles and another of varying particle size with constant β are taken in turn to determine the surface effect.

Results obtained are illustrated in Fig. 4. The solid lines in this figure are derived from the integral form of Eq. (1), that is

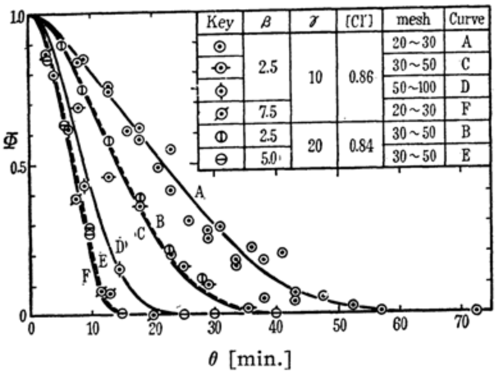

Fig. 4. Effect of the surface area of iron particles on the reaction rate.

$$\theta = -\int_{1.0}^{\Phi} \frac{\mathrm{d}\Phi}{(a_p + a_w)R} \tag{6}$$

where R is the standard reaction rate given as line A in Fig. 11. Agreement between the experimental results and the calculated lines seems to verify that the reaction rate is proportional to the surface area of iron particles.

Provided γ-value, the molal ratio of water to nitrocompound, is less than 6~7, the rate decreases steadily as the reaction proceeds.

The experimental results, however, verify the above conclusion as obvious from the lines B and C in Fig. 11.

c. Effect of Liquid Volume on the Reaction Rate.—Fig. 5 illustrates the effect of γ on the reaction rate under Φ-value of 0.5. If γ is larger than 6~7, the reaction proceeds smoothly and the rate is fairly constant, independent of changing γ.

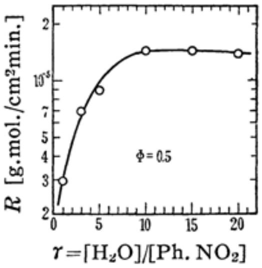

Fig. 5. Effect of the liquid bulk volume on the reaction rate.

This is supposed to mean that the reaction does not occur in the aqueous phase.

An increase in the volume of the oil layer also fails to improve the rate; in this case local reaction proceeds violently due to local overheating when the aqueous layer is decreased in volume compared with the oil layer.

In such an extreme case as when a theoretically required amount of water is used, even generation of ammonia vapor is observed.

This local phenomenon is supposed to be ascribed to insufficient removal of evolving reaction heat as a result of difficulty in vaporization of the co-existing water.

d. Reduction of Nitrobenzene with a Rotating Circular Iron Disk.—Nitrobenzene containing aniline in various proportions is reduced with a circular iron disk, made of mild steel, (80 mm. in dia., 6~7 mm. thick), with a center shaft, in order to determine whether the reaction proceeds mainly on the iron surface contacting with the aqueous phase or on that contacting with the oil layer.

This disk is rotated in any desired phase of oil or aqueous layer.

A reactor composed of flat-bottomed double glass cylinders of similar form is used and the annular space is filled with water boiling under atmospheric pressure. The inner cylinder has dimensions of 100 mm. dia., 250 mm. height, a capacity of about two liters.

Temperature of the reactants is maintained at 98°C. Prior to a run, the same volume of aqueous layer (1N-$FeCl_2$ solution) and that of oil layer (ratio of $Ph.NO_2$ to $Ph.NH_2$ is varied) are both preheated and charged to the height of 200 mm.

A circular iron disk etched with aqueous hydrochloric acid and washed with water is then placed in the axial position in a desired layer.

A low agitation speed of 550 r.p.m. is used to prevent intermixing of the separated aqueous and oil layers.

The reduction rate is expressed as the weight decrease of the disk, per unit surface area of the disk, per unit time. Fig. 6 illustrates the mean curves obtained from various runs when the disk is rotated in oil or in aqueous layer.

It is obvious from the figure that the overall rate of the reaction on the aqueous layer-iron interface is initially higher than that on the oil-iron interface, but there is no appreciable difference between the two in the final reduction stage.

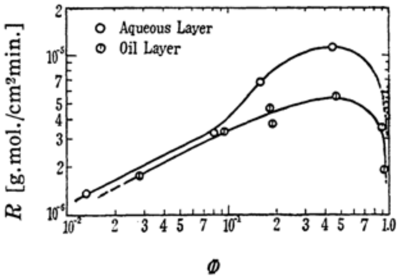

Fig. 6. R vs. Φ with the rotating disk.

In the initial reduction stage, an interesting phenomenon is observed when the disk is rotated in the oil layer, especially when the nitrobenzene content is much higher than the aniline content.

In this case, a hard black crust of Fe_3O_4 covers the disk uniformly and the progress of the reaction is retarded. This would probably be attributed to rapid oxidation of the surface oxide film of lower grade into a final form of ferroso-ferric oxide as a result of insufficient supply of water to the reaction interface due to low solubility of water into the nitrobenzene-rich oil layer. Such retardation due to crust formation is not observed in the water phase under the same conditions or in the final stage of the reduction.

The surface of the smoothly oxidized iron disk is composed of three layers-a thin surface oxide layer of loose structure, a middle thin layer consisting of very fine silvery iron grains and a ground iron layer beneath it.

These layers can easily be recognized by washing the disk with a gentle stream of water.

The existence of the layer of fine iron crystal grains seems to suggest that the reaction of the ground iron surface is liable to proceed along the intergranular zone between iron crystal grains.

In order to calculate R, the residual weight of the iron disk is weighed, for convenience sake, after the oxide crusts or the fine iron grains are all removed.

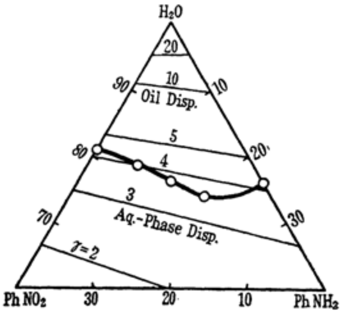

Fig. 7. Phase inversion

R given in Fig. 6 is therefore fairly overestimated in comparison with the value obtained from the batch reduction with iron particles.

e. *Effect of Phase Inversion.*—Fig. 7 illustrates the phase inversion caused by changing the compositions of the three component liquid mixture, $Ph.NO_2$–$Ph.NH_2$–1 N $FeCl_2$ aqueous, under the temperature of 100°C. If γ is larger than about four, the oil layer disperses into the aqueous layer to form stable droplets, when the reaction mixture is agitated.

This γ-value roughly corresponds to the critical condition determining the mechanical properties of the oxide sludge obtained from the oxidation of iron particles. If γ is larger than 4–5, an iron oxide sludge which has good filtering property is obtained, but even under the same condition, if the reaction does not proceed to completion, the iron oxide sludge has poor filtering property. Thus, the filtering properties of the oxide sludge seems to depend on the degree of completion of the reaction and the progress of the reaction seems to relate to the phase inversion. One probable explanation for this is that the volumetric ratio of oil to aqueous layer in the above case is much higher than that in the range where γ-value is lower than 4–5 (the equivolumetric point corresponds roughly to γ-value of 6–7) and that such phenomenon as crust formation on the iron particles retards the completion of the reaction.

f) *Some Considerations on the Reaction Zone.*—As obovious from the above-mentioned experiments, the reaction rate seems to be controlled by an overall process going on over the iron surface, because the reaction rate is in proportion to the surface area of iron particles. As illustrated in Fig. 3, no appreciable influence of rotation speed of the agitator is observed, provided the iron particles are fully fluidized into the liquid bulk.

If the rate of mass transfer between heterogeneous liquid phases has some influences on the reaction rate under such fluidized state, the rate should vary with (rotation speed)$^{3\sim5}$ [12]. Similarly, if the diffusion process of reactants through the liquid film formed on the surface of iron particles to the iron surface is the rate-determining step, the rate should vary with (rotation speed)$^{0.8}$ [13].

---

[12] A.W. Hixon and M.I. Smith, *Ind. Eng. Chem.*, **41**, 973 (1949): S. Yagi, T. Miyauchi and K. Kogure, *Chem. Eng. Japan*, **15**, 65 (1950).

[13] S. Nagata, *Chem. Eng. Japan*, **13**, 41 (1948). The exponent, 0.8 is determined by extraporation of Nagata's experimental correlation.

Thus, it seems to be reasonable to assume that the overall chemical (or may be physicochemical) process on the iron surface is the rate-determining step.

From the experimental results obtained with a rotating disk, it is also pointed out that the overall rate of the reaction on the water-iron interface is higher than the rate on the oil-iron interface in the initial stage of the reduction, but that there is no appreciable difference between the two in the final stage.

V-2. Effect of Some Physico-chemical Factors.—a. *Reaction Temperature.*—Fig. 8 illustrates the effect of varying reaction temperature under the following conditions

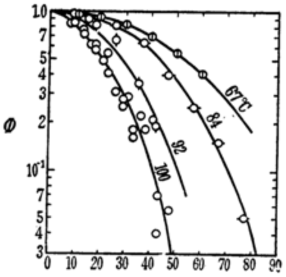

Fig. 8. Φ vs. θ under various temperature.

$\beta = 2.5$ [Cl′]=0.84 N
$\gamma = 10$ r. p. m.=1100
Size of iron particles=20–30 mesh.

Plotting of R vs. $1/T$ is shown in Fig. 9 under Φ of 0.3, because, in this range of Φ, the reaction proceeds, almost independent of the concentration of nitrocompound, that is, according to pseudo-zeroth-order.

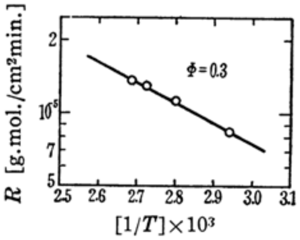

Fig. 9. R vs. $1/T$ (T in °K).

Apparent activation energy calculated is 3.66×10^3 cal./mol. which is unexpectedly small for the large exothermic reaction heat.

The color of oxide sludge also changes with reaction temperature as follows:

React. Temp. °C	60–67	75–84	85–95	100
Color of oxide sludge	pale yellow	reddish yellow	reddish brown	black

b. *Chlorine Iron Concentration.*—According to Lyons and Smith (5), 0.98 N of chlorine ion concentration (0.035 g. of Cl′ as $FeCl_3$ per ml.) gave the best result. Fig. 10 illustrates an example of our experiments with varying chlorine ion concentration under the following conditions:

$\beta = 2.5$ r. p. m.=1100
$\gamma = 10$ Reaction temp.=100°C
Size of iron particles=30–50 mesh.

It is observed that no appreciable improvement can be brought about if the chlorine ion concentration is greater than 0.8 N and that a rapid decrease in the reaction rate occurs for chlorine ion concentration when it is less than 0.8 N.

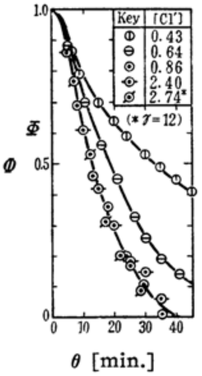

Fig. 10. Φ vs. θ under various chlorine ion concentrations.

V-3. Standard Reaction Rate.—On the above mentioned studies is established, for convenience' sake, a standard reaction rate at the boiling point of the reaction mixture under atomospheric pressure, the usual condition industrially applied. This is because the rate is proportional only to the surface area of iron particles employed, provided γ is larger than about 8 and [Cl′] is larger than 0.8 N. With experimental accuracy taken into consideration, the selected experimental condition will be,

$\beta = 2.5$ [Cl′]=0.86 N
$\gamma = 10$ Temp.=100°C
r. p. m.=1100
Size of iron particles=20–30 mesh.

Plotting of Φ vs. θ is illustrated as curve D in Fig. 12, and R, calculated by Eqs. (1) and (5) based on these data, is plotted in Fig. 11 as a function of Φ. The reaction rate is traced up to Φ of 10^{-4}, because aniline of this purity is usually employed both in industry and commerce. The curve is characterized as follows: the initial induction period is followed by zeroth-order behavior up to

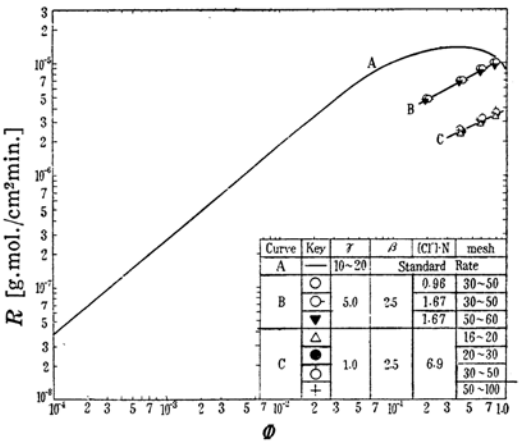

Fig. 11. Typical R vs. Φ.

Φ of 0.1, and then, in the final reaction stage, the slope of the reaction rate curve drops, roughly corresponding to that of the apparent first order reaction. These behaviors have also been confirmed experimentally with the continuous flow reactor. As mentioned above, this curve is employed to calculate θ in Eq. (6) and good agreement is obtained between calculated lines and experimental results as already illustrated in Fig. 4.

VI. Preparation of Various Primary Amines

The effects of surface area, chlorine ion concentration and molal ratio of water to nitrocompound are respectively examined using o-nitrotoluene.

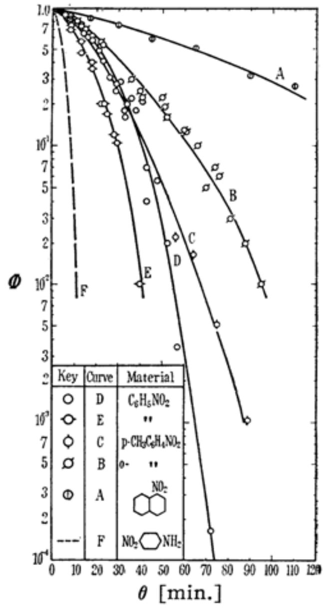

Fig. 12. Reduction rates of various mononitrocompounds $\beta=2.5$, $\gamma=10\sim15$, $[\mathrm{Cl}']=0.84\sim0.88\mathrm{N}$, reduction temp. $=100°\mathrm{C}$, r. p. m. $=1100$, size of iron particles $=30\sim50$ mesh (Curve D: $20\sim30$ mesh).

The results indicate that the reaction proceeds in a similar manner to those of nitrabenzene.

Fig. 12 illustrates the reduction rates of various mononitrocompounds under the conditions given in the figure. The rate curve of p-nitroaniline is assumed because the reaction proceeds too fast for us to measure the rate accurately.

Comparisons between the reaction rates of examined nitrocompounds by these curves lead us to conclude that there is a parallel relation between the overall reactivity and the mutual solubility of water and oil layers, although the latter is not yet accurately made clear. Moreover, there may be some influence of the chemical reactivity of each nitrocompound itself. More investigations are needed to solve these problems.

VII. General Conclusions

(1) As a fundamental approach to the continuous operation, the technical reaction rates of Bechamp's reduction have been studied, and it has become clear that the continuous process is industrially feasible.

(2) This reaction proceeds mainly according to the surface reaction mechanism on the iron surface, provided the iron particles are fully fluidized into the reaction mixture.

(3) Under the standard reaction conditions, the reduction of nitrobenzene largely proceeds according to the zeroth-order behavior after the initial induction period and according to the first-order in the final stage. In the stage of the zeroth-order behavior, the reaction occurs mainly on the aqueous layer-iron interface, but in the final stage reaction proceeds simultaneously on both water-iron interface and oil-iron interface.

(4) γ whose values are larger than 6–7 is suitable for smooth progress of the reaction.

(5) Apparent activation energy of the reduction of nitrobenzene is determined as 3.66×10^3 cal./mol. in the zeroth-order range.

(6) No appreciable difference in the reaction rate is observed when $[\mathrm{Cl}']$ is 0.8–2.7 N, but rapid decrease in the reaction rate is obserbed when $[\mathrm{Cl}']$ is smaller than 0.8 N.

(7) Various mono-nitrocompounds are also reduced under similar conditions. The reaction rate of each compound seems to have some parallel relationship with its own solubility in addition to its chemical reactivity.

Chemical Engineering Laboratoty, Faculty
of Engineering, The University
of Tokyo, Tokyo